Draft version September 24, 2009
Preprint typeset using LaTeX style emulateapj v. 08/13/06

MEETING THE SCIENCE GOAL OF DETECTING MOLECULAR GAS IN MILKY WAY GALAXIES AT $Z = 3$

D. Obreschkow, I. Heywood, S. Rawlings, D. Rigopoulou
Astrophysics, Department of Physics, University of Oxford, Keble Road, Oxford, OX1 3RH, UK
Draft version September 24, 2009

ABSTRACT

We address the science goal of the Atacama Large Millimeter/submillimeter Array (ALMA) to detect the CO lines of a Milky Way (MW) galaxy at redshift $z = 3$ by studying a sample of 2000 simulated galaxies, which resemble the MW at $z = 0$. This sample was drawn from S^3-SAX, a semi-analytic simulation of the neutral atomic (HI) and molecular (H_2) hydrogen in galaxies evolved on the cosmic structure of the Millennium dark matter simulation. In this sample of simulated MW-type galaxies we tackle the cosmic history of the continuum-subtracted emission lines of $^{12}C^{16}O$ and HI. In particular, we give numerical values for the sample averages of the line luminosities, line widths, and angular sizes of the MW-type galaxies at $z = 3$.

Subject headings: ALMA science goals

1. INTRODUCTION

Molecular hydrogen in space constitutes the sole crèche for the formation of new stars. Therefore, it is likely that observations of molecular gas at high redshift will reveal the mechanisms by which stars formed in early cosmic times and in galaxies much younger than those frequently mapped today.

Motivated by these perspectives, the first science goal of the future Atacama Large Millimeter/submillimeter Array (ALMA) is to "detect spectral line emission from CO or CII in a normal galaxy like the Milky Way at a redshift of $z = 3$, in less than 24 hours of observation." [1] In order to translate this science goal into technical requirements, it is necessary to clarify whether a "galaxy like the Milky Way at a redshift $z = 3$" means literally a galaxy like the Milky Way (MW) placed at a cosmological distance corresponding to $z = 3$ or rather a typical MW progenitor at $z = 3$. In the following, we assume that a "galaxy like the Milky Way at a redshift $z = 3$" refers to a typical MW progenitor at $z = 3$. This seems to be the more sensible interpretation in a study ultimately dedicated to the understanding of our own origin, but it complicates the situation, as we are now compelled to estimate the CO and CII line signature of a MW progenitor at $z = 3$.

In this paper, we shall use a set of simulated galaxies to analyze the continuum-subtracted line luminosities of the first ten emission lines in the rotational energy spectrum of the $^{12}C^{16}O$ molecule, as well as the approximate velocity widths and angular sizes of the CO distribution, in a well-defined sample of simulated MW progenitors at $z = 3$. For reference and comparison, we will also study the HI emission line.

2. THE SIMULATION

Our analysis relies on S^3-SAX [2] (Obreschkow et al. 2009a), a simulation of neutral atomic (HI) and molecular (H_2) hydrogen in galaxies. This simulation was mainly produced to assist the design of the Square Kilometer Array (SKA), a future radio array with strong capabilities to detect HI at high z.

The S^3-SAX simulation relies on the evolving density field of the Millennium dark matter simulation (Springel et al. 2005). The Millennium simulation resolves the dark matter halos of galaxies as low in mass as the small magellanic cloud (SMC) in a cubic comoving volume of $(500/h\,\mathrm{Mpc})^3$. The dimensionless Hubble parameter h, defined as $H_0 = 100\,h\,\mathrm{km\,s^{-1}\,Mpc^{-1}}$, was set equal to $h = 0.73$, and the other cosmological parameters were chosen as $\Omega_{\mathrm{matter}} = 0.25$, $\Omega_{\mathrm{baryon}} = 0.045$, $\Omega_\Lambda = 0.75$, $\sigma_8 = 0.9$.

In a post-processing, De Lucia & Blaizot (2007, see also Croton et al. 2006) studied the approximate evolution of idealized model-galaxies placed at the centers of the dark matter halos of the Millennium simulation. The global galaxy properties, such as dynamical mass, stellar mass, cold gas mass, and morphology, were evolved according to discrete, simplistic rules. This "semi-analytic" simulation resulted in a catalog of evolving and merging galaxies. The number of galaxies at a cosmological time of $13.7 \cdot 10^9$ yrs (i.e. at $z = 0$) is about $3 \cdot 10^7$, and each of these galaxies has a well-defined history of growing and discretely merging progenitor galaxies.

Obreschkow et al. (2009a) applied an analytic post-processing to the galaxies in the semi-analytic simulation in order to subdivide their cold gas masses into HI, H_2, and Helium. They also assigned realistic radial distributions and velocity profiles to the HI and H_2 components. Subsequently, Obreschkow et al. (2009b) introduced a model to assign approximate CO line luminosities to the molecular gas of each galaxy. This model attempts to account for the heating of molecular gas by starbursts, active galactic nuclei (AGNs), and the cosmic microwave background (CMB), as well as for aspects, such as different metallicities, overlap factors, and molecular cloud structures. The effect of the CMB as an observing background, which reduces the detectable line luminosities, was carefully accounted for. Based on this model, Obreschkow et al. (2009b) presented a prediction of the cosmic evolution of the CO luminosity functions (LFs) for the lowest ten rotational transitions of the $^{12}C^{16}O$ molecule.

Throughout this paper, we will assume that the radio and (sub)millimeter continuum can be perfectly subtracted, such that the line emission can be studied without considering the continuum. For other assumptions, limitations, and uncertainties of the S^3-SAX simulation, please refer to Section 6 in Obreschkow et al. (2009a) and Section 6.2 in Obreschkow et al. (2009b).

3. LINE EMISSION OF MW PROGENITORS AT HIGH Z

We shall now investigate the cosmic evolution of the CO and HI line signatures of the MW-type galaxies in the S^3-SAX simulation (see Section 2).

By definition (Obreschkow & Rawlings 2009a), we call a simulated galaxy at $z = 0$ a "MW-type", if its morphological type is Sb–Sc and if it matches the stellar mass M_*, the HI mass M_{HI}, the H_2 mass $M_{\mathrm{H_2}}$, the HI half-mass radius $r_{\mathrm{HI}}^{\mathrm{half}}$,

[1] all science goals at http://www.eso.org/projects/alma/
[2] online access at http://s-cubed.physics.ox.ac.uk

Quantity	Observed value ($z = 0$)	Ref.
Stellar mass	$M_s = 5^{+1}_{-1} \cdot 10^{10}\,M_\odot$	(a)
HI mass	$M_{HI} = 8^{+2}_{-2} \cdot 10^{9}\,M_\odot$	(b)
H_2 mass	$M_{H_2} = 3.5^{+1}_{-1} \cdot 10^{9}\,M_\odot$	(c)
HI half-mass radius	$r^{half}_{HI} = 15^{+5}_{-5}$ kpc	(b)
H_2 half-mass radius	$r^{half}_{H_2} = 7^{+1}_{-1}$ kpc	(c)

TABLE 1
OBSERVATIONAL ESTIMATES OF MW PROPERTIES (AT $z = 0$) WITH 1-σ UNCERTAINTIES, ADOPTED FROM: (A) FLYNN ET AL. (2006); (B) FROM ANALYTIC FITS TO $\Sigma_{HI}(r)$ IN KALBERLA & DEDES (2008); (C) FROM $\Sigma_{H_2}(r)$ IN TABLE 3 IN SANDERS ET AL. (1984).

Quantity	Value ($z = 3$)
Virial mass	$M_{vir} = 2.3^{+0.9}_{-0.7} \cdot 10^{11}\,M_\odot$
Stellar mass	$M_s = 5.3^{+3.9}_{-2.5} \cdot 10^{9}\,M_\odot$
HI mass	$M_{HI} = 0.7^{+1.1}_{-0.5} \cdot 10^{9}\,M_\odot$
H_2 mass	$M_{H_2} = 2.8^{+1.8}_{-1.3} \cdot 10^{9}\,M_\odot$
HI half-mass radius	$r^{half}_{HI} = 3.8^{+2.1}_{-1.6}$ kpc
H_2 half-mass radius	$r^{half}_{H_2} = 1.4^{+0.9}_{-0.7}$ kpc
HI line width (FWHM)	$w^{HI}_{50} = 260^{+50}_{-40}$ km s^{-1}
CO line width (FWHM)	$w^{CO}_{50} = 280^{+140}_{-50}$ km s^{-1}

TABLE 2
SAMPLE AVERAGES WITH 1-σ SCATTER FOR VARIOUS PROPERTIES OF 2000 SIMULATED MW-TYPE GALAXIES AT $z = 3$.

	Luminosity ($z = 3$)		Flux ($z = 3$)	
	[W]	[Jy km s^{-1} Mpc^2]	[W m^{-2}]	[Jy km s^{-1}]
HI	$1.7^{+2.5}_{-1.1} \cdot 10^{27}$	$3.7^{+5.6}_{-2.4} \cdot 10^{4}$	$2.1^{+3.2}_{-1.4} \cdot 10^{-28}$	$1.8^{+2.7}_{-1.1} \cdot 10^{-5}$
CO(1–0)	$1.0^{+1.3}_{-0.5} \cdot 10^{31}$	$2.8^{+3.5}_{-1.3} \cdot 10^{6}$	$1.3^{+1.6}_{-0.6} \cdot 10^{-24}$	$1.3^{+1.7}_{-0.6} \cdot 10^{-3}$
CO(2–1)	$8.5^{+11}_{-4.0} \cdot 10^{31}$	$1.2^{+1.6}_{-0.5} \cdot 10^{7}$	$1.1^{+1.4}_{-0.5} \cdot 10^{-23}$	$5.6^{+7.5}_{-2.6} \cdot 10^{-3}$
CO(3–2)	$2.6^{+3.8}_{-1.2} \cdot 10^{32}$	$2.4^{+3.5}_{-1.1} \cdot 10^{7}$	$3.3^{+4.8}_{-1.6} \cdot 10^{-23}$	$1.1^{+1.7}_{-0.5} \cdot 10^{-2}$
CO(4–3)	$4.6^{+8.9}_{-2.4} \cdot 10^{32}$	$3.2^{+6.1}_{-1.6} \cdot 10^{7}$	$5.9^{+11}_{-3.0} \cdot 10^{-23}$	$1.5^{+2.9}_{-0.8} \cdot 10^{-2}$
CO(5–4)	$5.3^{+17}_{-3.1} \cdot 10^{32}$	$2.9^{+9.1}_{-1.7} \cdot 10^{7}$	$6.7^{+21}_{-3.9} \cdot 10^{-23}$	$1.4^{+4.4}_{-0.8} \cdot 10^{-2}$
CO(6–5)	$4.3^{+22}_{-3.1} \cdot 10^{32}$	$2.0^{+10}_{-1.4} \cdot 10^{7}$	$5.5^{+28}_{-4.0} \cdot 10^{-23}$	$9.5^{+49}_{-6.9} \cdot 10^{-3}$
CO(7–6)	$2.8^{+23}_{-2.5} \cdot 10^{32}$	$1.1^{+9.2}_{-1.0} \cdot 10^{7}$	$3.6^{+30}_{-3.1} \cdot 10^{-23}$	$5.3^{+44}_{-4.7} \cdot 10^{-3}$
CO(8–7)	$1.6^{+19}_{-1.5} \cdot 10^{32}$	$5.4^{+65}_{-5.1} \cdot 10^{6}$	$2.0^{+25}_{-1.9} \cdot 10^{-23}$	$2.6^{+31}_{-2.4} \cdot 10^{-3}$
CO(9–8)	$7.9^{+130}_{-7.7} \cdot 10^{31}$	$2.4^{+38}_{-2.3} \cdot 10^{6}$	$10^{+160}_{-9.7} \cdot 10^{-24}$	$1.2^{+18}_{-1.1} \cdot 10^{-3}$
CO(10–9)	$3.4^{+75}_{-3.3} \cdot 10^{31}$	$9.3^{+200}_{-9.1} \cdot 10^{5}$	$4.3^{+95}_{-4.2} \cdot 10^{-24}$	$4.5^{+99}_{-4.4} \cdot 10^{-4}$

TABLE 3
AVERAGES WITH 1-σ SCATTER FOR THE HI AND CO LINE LUMINOSITIES AND FLUXES OF 2000 SIMULATED MW-TYPE GALAXIES AT $z = 3$. THESE LUMINOSITIES AND FLUXES ARE THOSE MEASURED AGAINST THE CMB, WHICH REPRESENTS AN IMPORTANT OBSERVING BACKGROUND AT $z = 3$ (SEE OBRESCHKOW ET AL. 2009B).

and the H_2 half-mass radius $r^{half}_{H_2}$ of the MW, given in Table 1, within a factor 1.3. This factor roughly matches the empirical uncertainties. According to this definition, the S^3-SAX simulation contains about 2000 MW-type galaxies at $z = 0$. At $z > 0$, we define MW-type galaxies as those objects, which are the most massive progenitors of a MW-type galaxy at $z = 0$.

The cosmic evolution of the sample averages of various properties of the simulated MW-type galaxies is shown in Figure 1; and the specific values at $z = 3$ have been summarized in Tables 2 and 3. The luminosity distance used for the conversion between luminosities and fluxes in Table 3 is $D_L = 25.7$ Gpc, corresponding to $z = 3$ with the cosmological parameters of Section 2. In order to convert the frequency-integrated line luminosities (here in units of W) into velocity-integrated luminosities (here in units of Jy km s^{-1} Mpc^2) or brightness temperature luminosities (e.g. units of K km s^{-1} pc^2) and to convert the frequency-integrated fluxes (here in units of W m^{-2}) into velocity-integrated fluxes (here in units of Jy km s^{-1}), please refer to Appendix A in Obreschkow et al. (2009b).

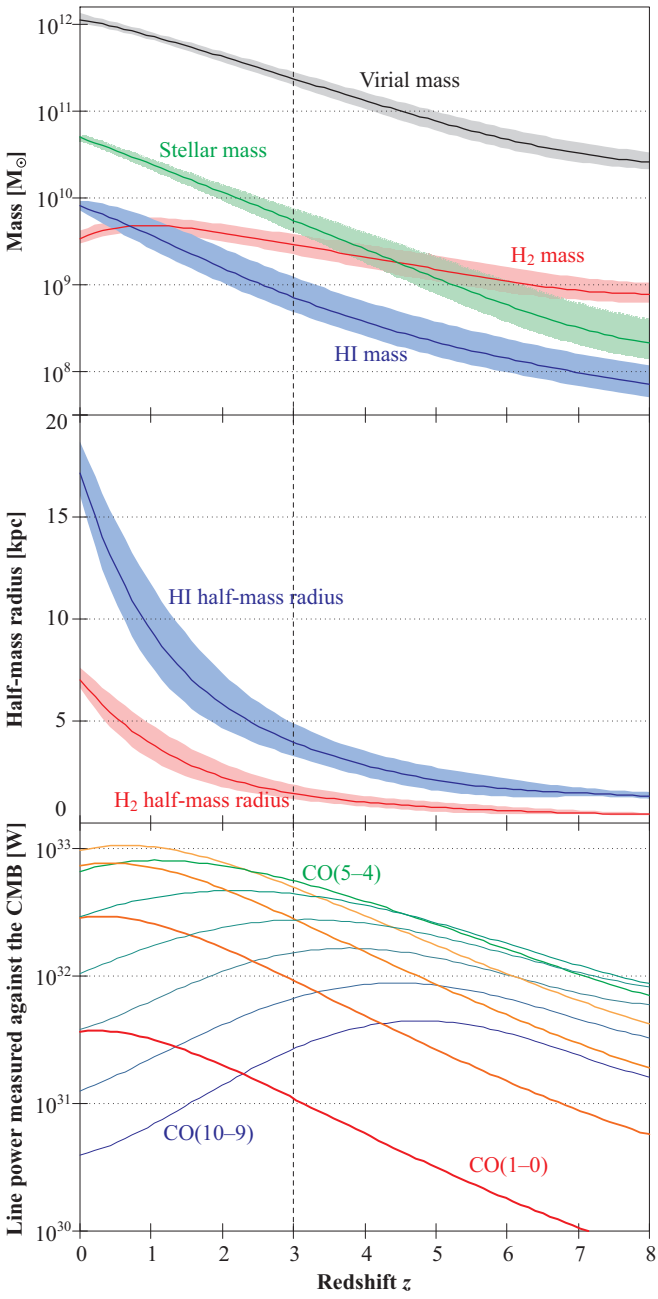

FIG. 1.— Cosmic evolution of the average galaxy properties of the 2000 simulated MW-type galaxies. The average values (solid lines) are *arithmetic* sample averages, even in the top and bottom panel, where a logarithmic scale was chosen to represent those averages. The shaded regions in the top panel and the middle panel represent the 0.5-σ scatter around the average values.

We emphasize that the sample size of 2000 MW-type galaxies at $z = 0$ decreases monotonically with z, since the different evolution scenarios of the MW-type galaxies start at different initial redshifts, depending on the local dark matter distribution. In other words, with increasing z, the average MW properties displayed in Figure 1 are increasingly biased towards the MW-type galaxies, which formed early in the history of the Universe. At $z = 3$ this is not an issue, since in 95% of all 2000 simulation scenarios the MW formed before $z = 3$.

However, only in 50% of all scenarios the MW formed before $z = 7$, and only in 20% it formed before $z = 8$.

Detailed physical interpretations of the cosmic evolution displayed in Figure 1 can be found in Obreschkow & Rawlings (2009b, evolution of the HI and H_2 masses), Obreschkow & Rawlings (2009a, evolution of the galaxy sizes), and Obreschkow et al. (2009b, evolution of the CO-luminosities). In brief, the radius of individual galaxies grows with cosmic time approximately as $(1+z)^{-1}$ (Bouwens et al. 2004; Trujillo et al. 2006; Buitrago et al. 2008), as a (not entirely understood) consequence of dark matter accretion (Gunn & Gott 1972). This size evolution is reflected in the evolution of the HI and H_2 radii (see Figure 1, middle panel), and it is responsible for an increase in the pressure of the interstellar medium (ISM) with z. The latter causes the H_2/HI mass ratio to increase with z, by virtue of the relation between the ISM pressure and the H_2/HI ratio (e.g. Elmegreen 1993; Blitz & Rosolowsky 2006; Leroy et al. 2008). This results in an essentially constant H_2 mass for the MW-type galaxies in the redshift range $z = 0-3$ (see Figure 1, top panel), although the total cold hydrogen mass (HI+H_2) decreases with z.

For the lower order CO transitions up to about CO(5–4), the observable line power decreases monotonically with z (see Figure 1, bottom panel). This is the combined effect of the evolving H_2 mass and the CMB, which presents a stronger observing background at high z, hence reducing the observable power. However, the higher order CO transitions of the MW-type galaxies, become more powerful with z, out to about $z \approx 2-5$. This behavior is due to the excitation of the higher energy levels by radiation from starbursts and AGNs. In the simulation, these heating effects are strongest in the range $z = 2-7$. However, the heating varies markedly amongst different galaxies, for example due to their different merger histories; therefore the scatter of the higher order CO luminosities in Table 3 is very large.

4. ACKNOWLEDGEMENTS

The Millennium Simulation databases used in this paper and the web application providing online access to them were constructed as part of the activities of the German Astrophysical Virtual Observatory.

REFERENCES

Blitz L., Rosolowsky E., 2006, ApJ, 650, 933
Bouwens R. J., Illingworth G. D., Blakeslee J. P., Broadhurst T. J., Franx M., 2004, ApJ, 611, L1
Buitrago F., Trujillo I., Conselice C. J., 2008, ArXiv e-prints
Croton D. J., et al., 2006, MNRAS, 365, 11
De Lucia G., Blaizot J., 2007, MNRAS, 375, 2
Elmegreen B. G., 1993, ApJ, 411, 170
Flynn C., Holmberg J., Portinari L., Fuchs B., Jahreiß H., 2006, MNRAS, 372, 1149
Gunn J. E., Gott J. R. I., 1972, ApJ, 176, 1
Kalberla P. M. W., Dedes L., 2008, A&A, 487, 951
Leroy A. K., Walter F., Brinks E., Bigiel F., de Blok W. J. G., Madore B., Thornley M. D., 2008, AJ, 136, 2782
Obreschkow D., Croton D., DeLucia G., Khochfar S., Rawlings S., 2009a, ApJ, 698, 1467
Obreschkow D., Heywood I., Klöckner H.-R., Rawlings S., 2009b, ApJ, 702, 1321
Obreschkow D., Rawlings S., 2009a, MNRAS, accepted
—, 2009b, ApJ, 696, L129
Sanders D. B., Solomon P. M., Scoville N. Z., 1984, ApJ, 276, 182
Springel V., et al., 2005, Nature, 435, 629
Trujillo I., et al., 2006, ApJ, 650, 18